

Modeling the collective magnetic behavior of highly-packed arrays of multi-segmented nanowires

This content has been downloaded from IOPscience. Please scroll down to see the full text.

2016 New J. Phys. 18 013026

(<http://iopscience.iop.org/1367-2630/18/1/013026>)

View [the table of contents for this issue](#), or go to the [journal homepage](#) for more

Download details:

IP Address: 158.109.56.165

This content was downloaded on 11/01/2016 at 17:35

Please note that [terms and conditions apply](#).



PAPER

Modeling the collective magnetic behavior of highly-packed arrays of multi-segmented nanowires

OPEN ACCESS

RECEIVED

31 August 2015

REVISED

24 November 2015

ACCEPTED FOR PUBLICATION

15 December 2015

PUBLISHED

11 January 2016

Original content from this work may be used under the terms of the [Creative Commons Attribution 3.0 licence](#).

Any further distribution of this work must maintain attribution to the author(s) and the title of the work, journal citation and DOI.

S Agramunt-Puig¹, N Del-Valle¹, E Pellicer¹, J Zhang¹, J Nogués^{2,3}, C Navau¹, A Sanchez¹ and J Sort^{1,3}¹ Departament de Física, Universitat Autònoma de Barcelona, E-08193 Bellaterra, Barcelona, Catalonia, Spain² Catalan Institute of Nanoscience and Nanotechnology (ICN2), CSIC and The Barcelona Institute of Science and Technology, Campus UAB, Bellaterra, E-08193 Barcelona, Spain³ Institució Catalana de Recerca i Estudis Avançats (ICREA), Barcelona, Catalonia, SpainE-mail: Alvar.Sanchez@uab.cat

Keywords: nanowires, micromagnetics, nanomagnetism

Abstract

A powerful model to evaluate the collective magnetic response of large arrays of segmented nanowires comprising two magnetic segments of dissimilar coercivity separated by a non-magnetic spacer is introduced. The model captures the essential aspects of the underlying physics in these systems while being at the same time computationally tractable for relatively large arrays. The minimum lateral and vertical distances rendering densely packed weakly-interacting nanowires and segments are calculated for optimizing their performance in applications like magnetic sensors or recording media. The obtained results are appealing for the design of multifunctional miniaturized devices actuated by external magnetic fields, whose successful implementation relies on achieving a delicate balance between two opposing technological demands: the need for an ultra-high density of nanowires per unit area and the minimization of inter-wire and inter-segment dipolar interactions.

Owing to their anisotropic shape and reduced lateral sizes, one-dimensional nanostructures (e.g., nanowires, nanotubes or nanorods) have boosted a wealth of applications in diverse technological areas, such as electronics and optoelectronics, magnetic memory units, biological sensors, gas sensors, spintronic devices or micro-/nano-electro-mechanical systems, amongst others [1–3]. The elongated shape of these nano-objects promotes mutual interactions along preferential directions when these structures are arranged or assembled together to form an array, hence leading to physical properties that are highly anisotropic.

An additional advantage of nanowires with respect to isotropic nanoparticles is that it is relatively easy to sequentially grow and combine various segments of dissimilar materials, each exhibiting different physico-chemical properties, along the length of the nanowire [1, 4, 5]. This renders multifunctionality to the obtained hybrid materials. Without being exhaustive, some recent examples of this type of materials are: Au/polypyrrole/Ni nanowires that simultaneously contain a biofunctionalizable segment (Au) and a ferromagnetic segment (Ni) that allows magnetic alignment and wireless manipulation [6]; Co/Cu and FeCoNi/Cu multilayered (barcode) nanowires displaying giant magnetoresistance (GMR) effect, suitable for magnetic field sensors and spintronic nanodevices [7–10]; Ag/ZnO nanowires suitable for photocatalysis, photochemical conversion and hydrogen generation [11]; CdTe/Au/CdTe trilayered nanowires for detection of DNA molecules [12]; FeCo/Cu barcode nanowires for magnetic control of biomolecule desorption [13]; Ni/CoPt exchange coupled patterned media [14, 15]; multilevel recording [16, 17] and so on. The progress in all these applications has been possible due to the tremendous advancement in the various synthetic methods to fabricate hybrid nanowires, including electrodeposition inside the pores of hard templates, electrospinning, or one-dimensional conjugation of building blocks (e.g., nanoparticles) [1, 5].

In terms of magnetic applications, the use of arrays of multi-segmented nanowires instead of multilayered magnetic continuous films is appealing for several reasons: (i) GMR elements with current-perpendicular-to-plane geometry can be easily fabricated in high-aspect ratio structures (such as nanowires) [18], minimizing the variation of the intralayer thicknesses, which is detrimental for the GMR effect; (ii) a large number of segments

with uniform thickness can be obtained in a fast and inexpensive way using pulse electrodeposition, thus enhancing the GMR effect by virtue of the increase in the number of magnetic layers with antiparallel orientation; (iii) a high areal density of multiplex sensors can be prepared for the simultaneous detection of several chemical agents, in the form of miniaturized devices. In all these cases, though, it is of utmost importance to be able to fully control the orientation of the different magnetic segments comprising the nanowires. This is possible by the use of external magnetic fields, provided that each magnetic segment exhibits a well-defined, sufficiently different, coercivity value. However, if the inter-wire lateral distance and/or the separation between the magnetic segments inside each nanowire are exceedingly small, then dipolar magnetic interactions are enhanced and can cause undesirable magnetic switching and concomitant loss in the functionality of the hybrid nanowires. Dipolar interactions are indeed detrimental for the magnetic stability of the multi-segmented nanowires, since the magnetic switching of one layer or nanowire may accidentally switch the neighboring ones. Hence, a clear understanding of the effects of magnetic interactions as a function of the geometrical arrangement of the hybrid nanowires is indispensable to optimize their performance. However, this problem is difficult to be theoretically tackled by conventional micromagnetic simulations, because the computation time drastically rises as the number of simulated ferromagnetic elements is progressively increased [19]. Hence there is an increasing need to develop new, time-saving, models to simulate the collective behavior large arrays of complex nanowires.

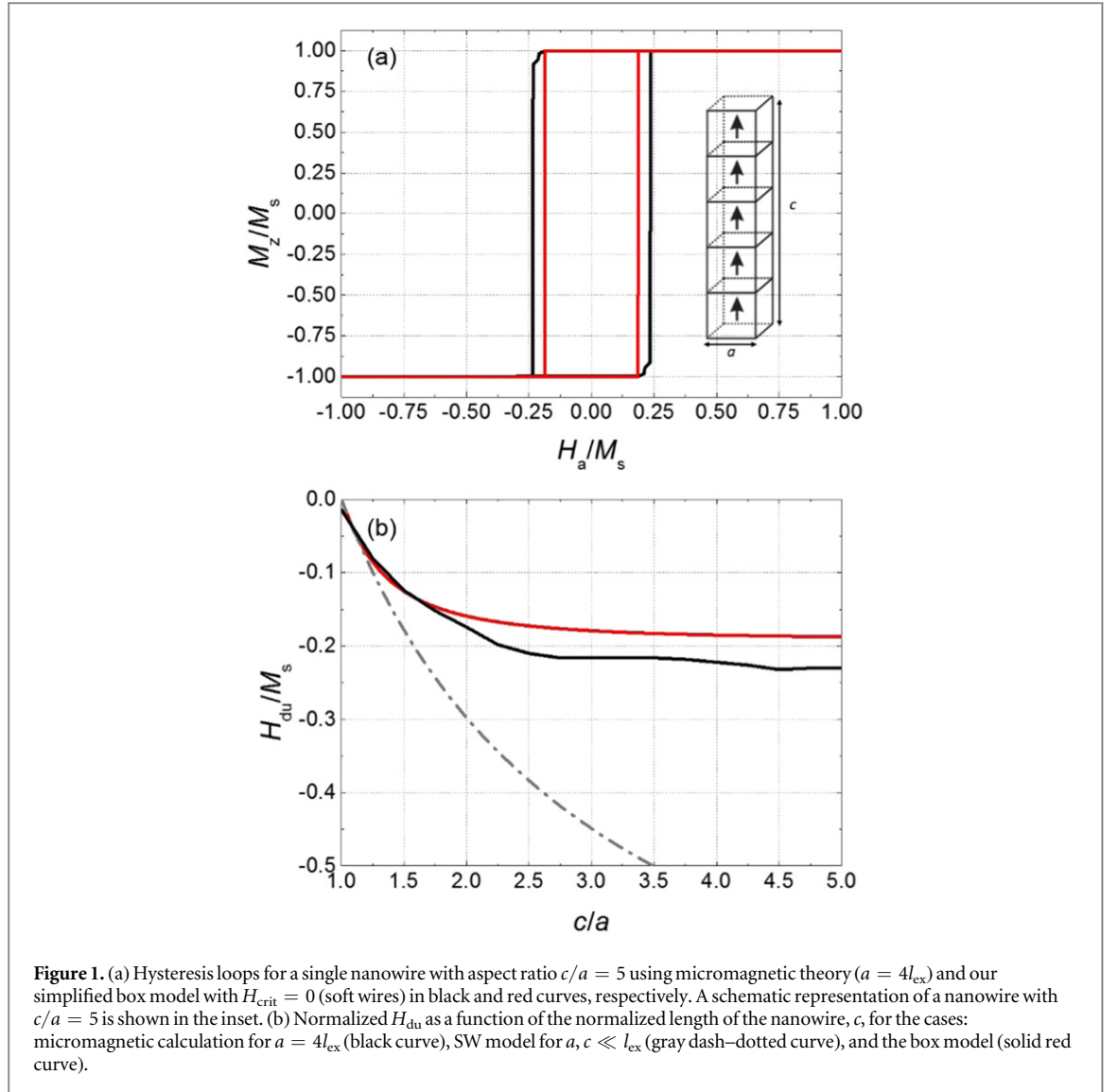
In this article we introduce an efficient model to simulate the collective magnetic behavior of large arrays of multi-segmented nanowires with a high aspect-ratio (length-to-diameter ratio, $c/a = 5$). This model is based on a coarse discretization of the nanowires in boxes, each considered as a single magnetic dipole, interacting magnetostatically with the other boxes. After validating the approximations by comparison with more accurate calculations (i.e., analytic and micromagnetics), we study the magnetic response of large arrays of nanowires, including the case of segmented wires. The results show that stable, well-defined, magnetization states can be obtained, provided that the wires are approximately separated in the horizontal direction a distance 1.5–2 times their diameter and the segments are about one diameter apart in the vertical direction (depending on the anisotropy of the hard phase).

The reversal modes of single nanowires have been studied widely in the literature [20–25]. Analytical calculations evidence, depending on the relation between the exchange length (l_{ex}) and the length-to-diameter ratio, two main reversal modes, coherent rotation and curling, although more advanced analyses have shown the possibility of reversal by nucleation of transverse domain walls [26–28]. Moreover, micromagnetic simulations have demonstrated other reversal modes like nucleation, propagation and annihilation of 3D vortex states [29, 30].

In arrays of such nanowires the field at which the magnetization deviates from uniformity, H_{du} , is particularly complex to study since it must be calculated over each of them and taking into account the whole ensemble of nanowires. Analytic studies assuming hexagonal arrangement of nanowires have shown the need for adding an additional term to the H_{du} of a single nanowire [20, 31]. This term may be interpreted as an average of the magnetostatic field and thus it depends linearly on the saturation magnetization and the density of nanowires [32] (e.g., the porosity of the template used to fabricate them [33]). This magnetostatic field reduces the H_{du} predicted for coherent and curling modes in single nanowires [20]. Other methods involve calculating the field of neighboring nanowires using accurate methods, but describing the field of further wires as a continuum [34, 35]. Micromagnetic calculations have been performed considering few nanowires [36] or applying periodic conditions to the algorithm [37]. In spite of these efforts, reliable tools to systematically scale up to a representative large number of nanowires are still lacking.

We first consider a nanowire with the shape of a prism with square base of side a and length c (see inset in figure 1(a)). The nanowire is divided into cubic boxes of side a , with a dipole of magnitude $M_S a^3$ in the middle of each box, where M_S is the saturation magnetization of the material. We assume that the whole nanowire is uniformly magnetized either in the positive or negative z direction (along the c direction) and we evaluate the total field at the center of each box, that is the sum of the applied field and magnetostatic fields created by all other boxes in the same nanowire and in neighboring nanowires. The magnetization of the nanowire switches when the maximum (in absolute value) of the z component of the total field is opposed to the overall nanowire magnetization and is larger than a certain threshold H_{crit} . This criterion can be mathematically formulated as follows. All boxes have the same magnetization $\vec{M} = \pm M_S \hat{z} = M \hat{z}$ and the field created by the j box at the center of the i box is $\vec{H}_{ij} = H_{ij} \hat{z} = \frac{M a^3}{2\pi d_{ij}^3} \hat{z}$, where d_{ij} is the distance between the centers of boxes i and j . Since the applied field is $\vec{H}_a = H_a \hat{z}$, the total field at the center of the i box is

$$\vec{H}_i = \vec{H}_a + \sum_{j \neq i} \vec{H}_{ij} = (H_a + \sum_{j \neq i} H_{ij}) \hat{z} = H_i \hat{z}. \quad (1)$$



If k is the box where $|H_i|$ is maximum for all i , then the magnetization of the nanowire switches when $|H_k| > H_{\text{crit}}$ and $\text{sign}(H_k) = -\text{sign}(M)$.

When this criterion is fulfilled, all the boxes of the nanowire switch together. The parameter H_{crit} takes implicitly into account the anisotropy of the involved materials. In the case of ideally soft (i.e., no magneto-crystalline anisotropy) nanowires, for simplicity, we assume $H_{\text{crit}} = 0$. For the case of hard (large magneto-crystalline anisotropy) nanowires this threshold is taken of the order of saturation magnetization M_S , $H_{\text{crit}} \sim M_S$ (similar to [38] for hard magnetic materials). One could choose Fe and CoPt as soft and hard ferromagnetic materials, respectively, as examples of actual materials.

The weaker magnetostatic field (in absolute value) is at the wire edges [39] (having less neighboring boxes), so H_{du} of an isolated soft nanowire is equal to the magnetostatic field at a box at the tip of the wire. This can be calculated as the sum of the magnetostatic fields that all the cells (with a magnetic dipole each one) create to the one at the edge, which can be analytically calculated as

$$\begin{aligned}
 \frac{H_{\text{du}}}{M_S} &= \frac{H_1}{M_S} = \sum_{j=2}^{c/a} \frac{a^3}{2\pi d_{1j}^3} = \sum_{j=2}^{c/a} \frac{a^3}{2\pi |\vec{r}_1 - \vec{r}_j|^3} \\
 &= \sum_{j=2}^{c/a} \frac{a^3}{2\pi |z_1 - z_j|^3} = \sum_{j=2}^{c/a} \frac{a^3}{2\pi ((j-1)a)^3} \\
 &= \frac{1}{2\pi} \sum_{j=2}^{c/a} \frac{1}{(j-1)^3} = \frac{1}{4\pi} \left[\phi\left(\frac{c}{a}\right) + 2\zeta(3) \right], \tag{2}
 \end{aligned}$$

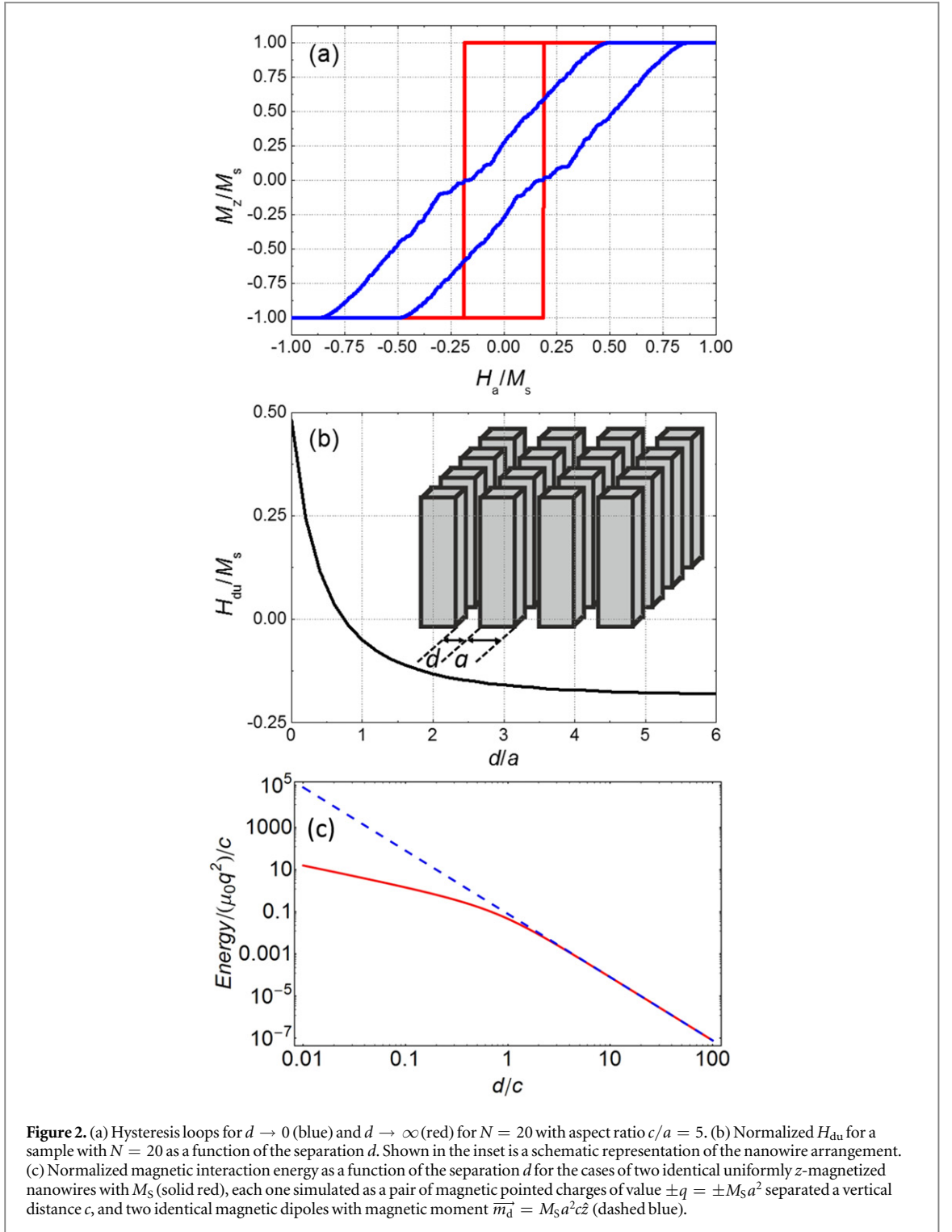
where we have chosen the origin of coordinates at the center of the top box of the nanowire, so the each box is placed at $\vec{r}_i = z_i \hat{z} = -(i-1)a \hat{z}$ with $i = 1, \dots, c/a$, and where $\phi(x)$ and $\zeta(x)$ are Polygamma function of

second order and the Riemann Zeta function, respectively. This expression can be obtained from equation (1) by setting $H_a = 0$ and $i = 1$, where 1 corresponds to the index of the edge box and c/a the number of the boxes in the NW. In figure 1 we analyze the case of an isolated nanowire. Figure 1(a) compares the results of this simple box model for soft nanowires ($H_{\text{crit}} = 0$) having aspect ratio $c/a = 5$ with a micromagnetics simulation [40] (using $a = 4l_{\text{ex}}$, where $l_{\text{ex}} = \sqrt{\frac{2A}{\mu_0 M_S^2}}$ and A is the exchange stiffness constant). Note that, although we consider $H_{\text{crit}} = 0$, the soft nanowire simulated by the box model has some coercivity due to the shape anisotropy. Namely, at zero-applied field, the total field (now only the magnetostatic field created by all the boxes of the nanowire) has the same direction as the magnetization of nanowire, thus there is no switching despite the $H_{\text{crit}} = 0$. Consequently, an extra field of opposite direction is required to overcome the dipolar field and hence induce the switching.

As seen in figure 1(a), the hysteresis loops calculated using micromagnetics and our simple box model are rather similar. Moreover, in the micromagnetics case, the deviation from uniformity field H_{du} and the switching field (field at which the magnetization switches its direction) are nearly the same. This allows considering only uniform states during the nanowire magnetization reversal in the box model, and therefore the only parameter that characterizes each hysteresis loop is H_{du} . To further verify the validity of our model, in figure 1(b) we plot the normalized deviation from uniformity field H_{du}/M_S as a function of the aspect ratio c/a of the nanowire using micromagnetics (assuming $a = 4l_{\text{ex}}$), and the box model using equation (2). For reference, we also plot the case $c, a \ll l_{\text{ex}}$, corresponding to the classical Stoner–Wohlfarth (SW) case [41], in which the magnetization remains uniform due to the large exchange interaction (only valid if the nanowire has very small dimensions). All calculations converge to the same $H_{\text{du}} = 0$ when the nanowire becomes a cube ($c = a$), because in this case the magnetostatic energy does not depend on the magnetization direction (i.e., no shape anisotropy). For larger c/a , H_{du} increases because of the difference in magnetostatic energy between the magnetization parallel and perpendicular to the wire, as predicted in [41]. For all aspect ratios, the largest (negative) H_{du} corresponds to the SW limit in which not only the magnetization is uniform, as in the box model, but also the demagnetizing field is. Micromagnetic calculations allow for small deviations of the magnetization (e.g., the formation of 3D flower states at the edges of the wires), therefore decreasing the magnetostatic energy of the nanowire (with respect to the uniform case). This results in a reduction of the switching field with respect to the SW model. Interestingly, the H_{du} obtained from the simpler box model roughly follows the trend of the micromagnetic calculations in the whole range of c/a , although it shows a slightly smaller H_{du} field since it only considers the field at the edges of the nanowires (where it is weaker). However, the predicted H_{du} is reasonably similar to the one calculated with micromagnetics for the whole c/a range. These results justify the use of our simple box model instead of tedious micromagnetic calculations to undertake the analysis of the switching behavior of large arrays of nanowires. Actually, the computation time of both models depends mainly on the evaluation of the magnetostatic field over all the elements and it is thus proportional to the square of their number. Micromagnetic boxes have a typical length $\sim l_{\text{ex}}$ (or smaller) [42, 43]. Instead, our model assumes that each box is a cube with side $\Delta_{\text{box}} = a$. Therefore, there are $(a/l_{\text{ex}})^3$ more micromagnetic cells than boxes, and as a consequence the calculation time when using the box model is reduced by a factor $(a/l_{\text{ex}})^6$. This implies that while the box model can treat a very large number of wires, the same arrangements turn computationally impossible to be treated by micromagnetics.

Next, we consider regular square arrays of $N_x \times N_y$ nanowires, with $N_x = N_y = N$, separated by a distance d along x and y directions (see sketch in figure 2(b)). Starting from large (positive) applied fields, all the nanowires are initially magnetized in the same direction. Each wire experiences a negative field along z due to the magnetostatic interaction with the rest of the wires, which will depend on the distance between them. In general, the overall magnetostatic field has a maximum (in absolute value) at the central nanowire (assuming N odd); therefore this wire is the one that switches first and determines H_{du} of the whole array. In figure 2(b) we show H_{du} for an $N = 20$ arrangement as a function of the inter-wire distance. When the nanowires get closer to each other ($d \rightarrow 0$) the switching field is large and positive, in the same direction as the initial magnetization. As the distance between nanowires is increased, their interaction becomes weaker and the deviation from uniformity field becomes negative, tending to the value for an isolated nanowire when d is large (see figure 1(b)). In particular, the magnetic interaction energy between two identical nanowires decreases with d and follows the dipole–dipole interaction dependence $1/d^3$ for $d > 2c$ ($d > 10a$) giving negligible long-range interaction values (see figure 2(c)) in agreement with figure 2(b). Similar results were analytically predicted by Guslienko [44] in in-plane magnetized circular cylindrical dot arrays. Interestingly, the shape of the hysteresis loops of the arrays changes considerably with d compared to the one of isolated nanowires. The loops are no longer squared but tilted, as depicted in figure 2(a).

We now consider segmented nanowires with a magnetically soft segment ($H_{\text{crit}} = 0$) and a hard segment ($H_{\text{crit}} = 3/4M_S$), both with aspect ratio $c/a = 5$. The saturation magnetization for the hard segment is M_S and for the soft one is $2M_S$, so when the whole nanowire is uniformly magnetized its overall saturation magnetization



is $M_T = 3M_S/2$. Shown in figure 3(a) is the loop for a single segmented wire where two segments are infinitely separated along the wire ($d_z \rightarrow \infty$), so that they do not interact magnetostatically. The hysteresis loop is simply the weighted sum of their individual loops, where the first and second jumps correspond to the reversal of the soft and hard segments, respectively. As can be seen in figure 3(b), for a single segmented wire when the two segments are in close proximity but not in contact (i.e., $d_z \rightarrow 0$, interacting magnetostatically but neglecting exchange effects), the loop shows a very slightly increase in the switching field of the soft part and an appreciable decrease in the switching field of the hard part with respect to the non-interacting case ($d_z \rightarrow \infty$). In the interacting case, when saturated in a positive applied field the box that feels a weaker field in the soft part is the one away from the interface. Thus, the field at this cell determines the switching field, which increases only slightly because the field exerted by the hard segment over it is relatively weak and in the same direction as the magnetization. In contrast, once the soft segment has switched, the weaker magnetostatic field over the hard

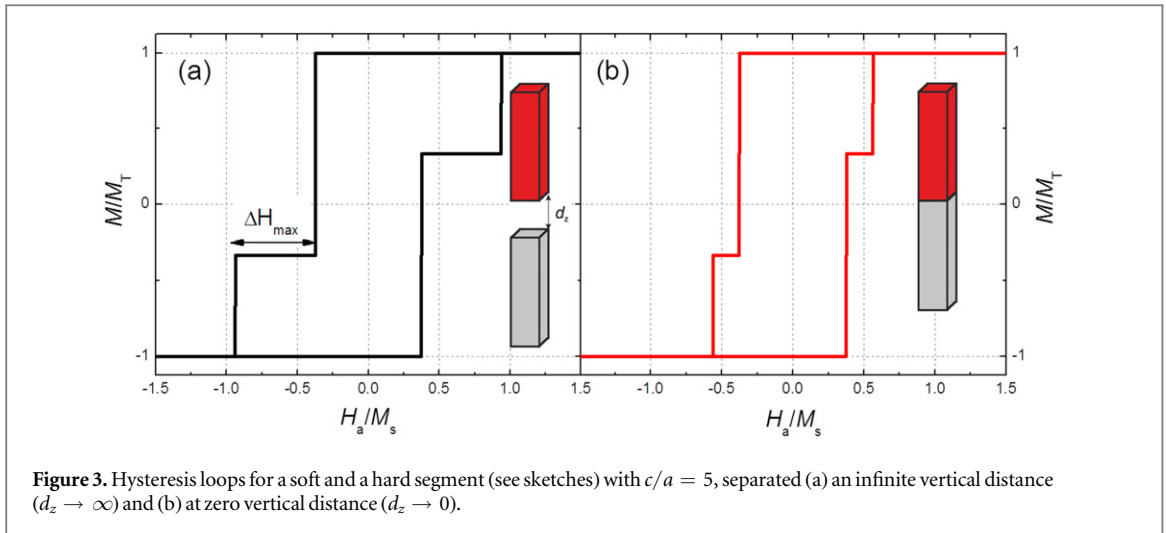


Figure 3. Hysteresis loops for a soft and a hard segment (see sketches) with $c/a = 5$, separated (a) an infinite vertical distance ($d_z \rightarrow \infty$) and (b) at zero vertical distance ($d_z \rightarrow 0$).

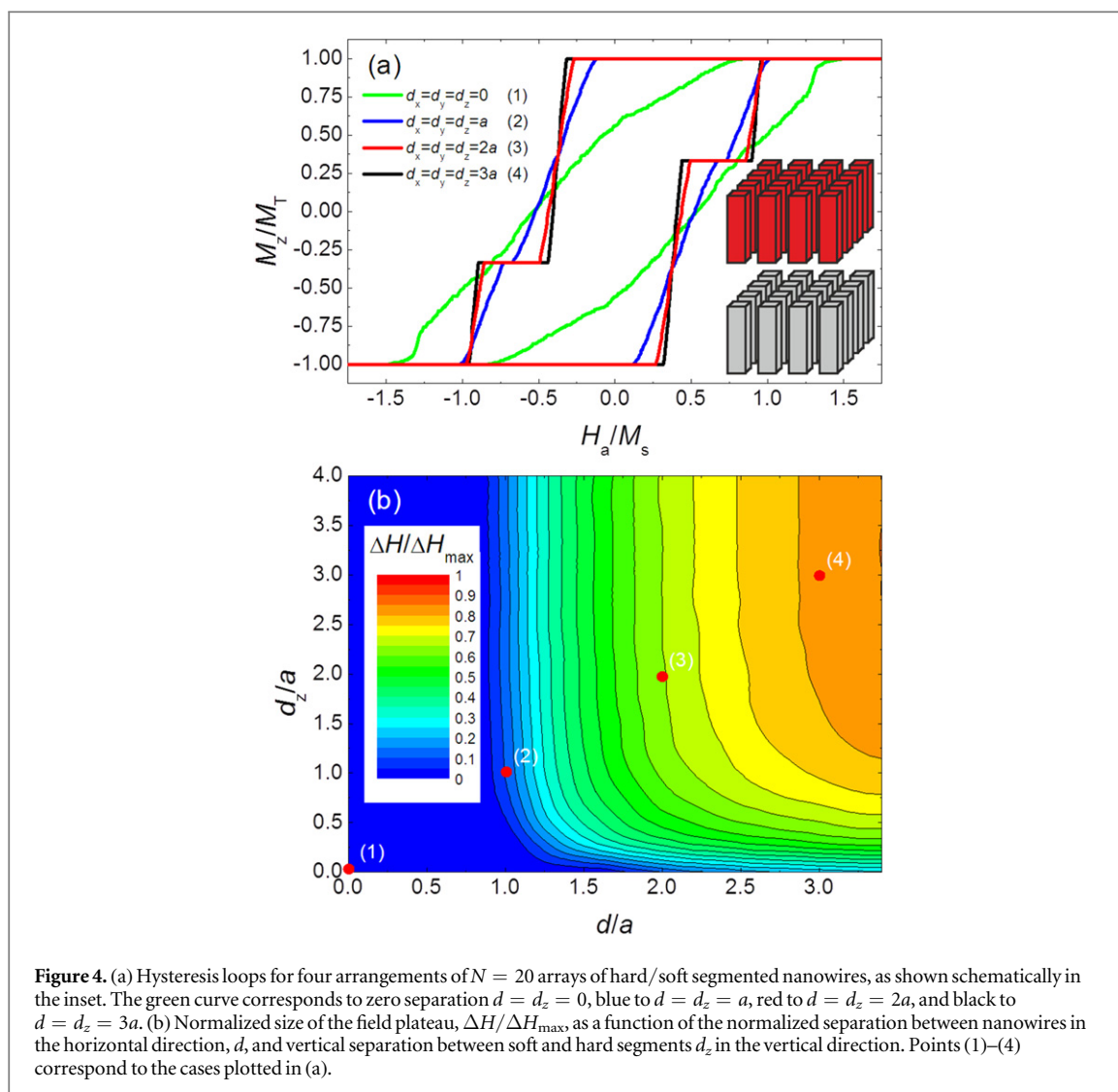
segment is in the interfacial box because of its proximity to the negatively magnetized soft segment, thus, the soft segment induces a field opposite to the magnetization of the hard segment therefore reducing its H_{du} .

To evaluate the feasibility to obtain multiple well-defined states using segmented wires, arrays of nanowires consisting of a soft and a hard segment (sketched in figure 4(a)) are considered. To optimize the design of the composite material, we analyze in a systematic way the effect of the in-plane distance of the wires in the array, d , and the distance between the soft and hard segments in each nanowire, d_z . As can be seen in figure 4(a), when their separation is large ($d \geq 2a$) the loop is almost the same as in figure 3(a), with well-established states, thus suitable for applications requiring multiple-states. However, for very small distances the loop radically changes as a consequence of the interactions among the wires and their segments, leading to a rounded shape, not useful for most technological uses. To establish the boundary of d and d_z to attain two well-defined states in each hysteresis sub-loop we use the width of the plateau ΔH in the hysteresis loop as a quality parameter. To normalize it, we divide ΔH by its maximum possible value, ΔH_{max} , i.e., when all segments are completely isolated (see figure 3(a)). In figure 4(b) we show $\Delta H/\Delta H_{max}$ for different in-plane (d) and out-of-plane (d_z) separations. It can be seen that for inter-wire distances below $d/a = 1$ the loop has no step, i.e., $\Delta H/\Delta H_{max} \sim 0$, thus, unusable for most purposes. If we set $\Delta H/\Delta H_{max} \sim 0.5$ as an indispensable requirement for a stable state, the minimum d suitable for applications would be about $1.5a$ (for moderate d_z). On the other hand, the system is less sensitive to the vertical separation d_z between wires. For example, for $d = 2a$ we would need only $d_z = 0.5a$ to fulfill the $\Delta H/\Delta H_{max} \sim 0.5$ criterion. These results indicate that the magnetostatic interaction from vertically separated segments is weaker than that for horizontal ones.

If the anisotropy of the hard segments is increased, for example by increasing the threshold to $H_{crit} = M_s$, we obtain a figure similar to figure 4(b) but with larger values of $\Delta H/\Delta H_{max}$ (not shown). The general trends are similar to figure 4(b) although the data is shifted to the left and down, that is, for $d = 2a$ and $d_z = 0.5a$ we obtain $\Delta H/\Delta H_{max} \sim 0.7$. Consequently, to fulfill $\Delta H/\Delta H_{max} \sim 0.5$ criterion only $d = 1.5a$ and $d_z = 0.25a$ would be necessary for this higher anisotropy case. Hence, in principle, designing multi-level nanowires with higher anisotropies of the hard counterpart would be desirable to increase the magnetic stability while safely operating the system. However, the maximum field available from the electromagnetic coils to establish the orientation of the hard layer would set the limit for the maximum allowable anisotropy.

In conclusion, we have presented a simple but powerful model to describe the magnetization switching of large arrays of segmented nanowires. Our model is capable of predicting the distances over which nanowires do not interact appreciably with their neighbors (horizontal separation $d > a$). At the same time we demonstrate that nanowires made of segments of different coercivity and saturation magnetization can be used to attain antiparallel or parallel magnetic alignment, as required in magnetic sensors based on the GMR effect and other applications based on multiple-states. Thus, the model can become a useful tool to efficiently design future optimized spin-valve like sensors or even other applications, such as high-density multi-level recording media or magnetic encoders.

We acknowledge the support from the 2014-SGR-1015 and 2014-SGR-150 projects of the Generalitat de Catalunya, the MAT2012-35370 and MAT2014-57960-C3-1-R projects from the Spanish Ministerio de Economía y Competitividad (MINECO)-the latter cofinanced by the 'Fondo Europeo de Desarrollo Regional' (FEDER)-, the SPIN-PORICS 2014-Consolidator Grant (Grant Agreement 648454) from the European Research Council (ERC), and the MANAQA project (grant agreement 296679) from the European Community's Seventh Framework Programme (FET-Open/FP7/2007-2013). AS acknowledges funding from



an ICREA Academia award. EP acknowledges the Spanish Ministerio de Economía y Competitividad (MINECO) for the ‘Ramon y Cajal’ contract (RYC-2012-10839). ICN2 acknowledges support from the Severo Ochoa Program (MINECO, Grant SEV-2013-0295).

References

- [1] Yuan J, Xu Y and Müller A H E 2011 One-dimensional magnetic inorganic-organic hybrid nanomaterials *Chem. Soc. Rev.* **40** 640–55
- [2] Wanekaya A K, Chen W, Myung N V and Mulchandani A 2006 Nanowire-based electrochemical biosensors *Electroanalysis* **18** 533–50
- [3] Krahn R, Morello G, Figuerola A, George C, Deka S and Manna L 2011 Physical properties of elongated inorganic nanoparticles *Phys. Rep.* **501** 75
- [4] Lee W, Scholz R, Nielsch K and Gösele U 2005 A template-based electrochemical method for the synthesis of multisegmented metallic nanotubes *Angew. Chem.* **117** 6204–8
- [5] Hurst S J, Payne E K, Qin L and Mirkin C A 2006 Multisegmented one-dimensional nanorods prepared by hard-template synthetic methods *Angew. Chem. Int. Ed.* **45** 2672–92
- [6] Bangar M A, Hangarter C M, Yoo B, Rheem Y, Chen W, Mulchandani A and Myung N V 2009 Magnetically assembled multisegmented nanowires and their applications *Electroanalysis* **21** 61–7
- [7] Pullini D and Busquets-Mataix D 2011 Electrodeposition efficiency of Co and Cu in the fabrication of multilayer nanowires by polymeric track-etched templates *ACS Appl. Mater. Interfaces* **3** 759–64
- [8] Cox B, Davis D and Crews N 2013 Creating magnetic field sensors from GMR nanowire networks *Sensors Actuators A* **203** 335–40
- [9] Piraux K, George J M, Despres J F, Leroy C, Ferain E, Legras R, Ounadjela K and Fert A 1994 Giant magnetoresistance in magnetic multilayered nanowires *Appl. Phys. Lett.* **65** 2484–6
- [10] Liu K, Nagodawithana K, Searson P C and Chien C L 1995 Perpendicular giant magnetoresistance of multilayered Co/Cu nanowires *Phys. Rev. B* **51** 7381–4(R)
- [11] Maijenburg W, Rodijk E J B, Maas M G, Enculescu M, Blank D H A and ten Elshof J E 2011 Hydrogen generation from photocatalytic silver/zinc oxide nanowires: towards multifunctional multisegmented nanowire devices *Small* **7** 2709–13
- [12] Wang X and Ozkan C S 2008 Multisegment nanowire sensors for the detection of DNA molecules *Nano Lett.* **8** 398–404

- [13] Ozkale B et al 2015 Multisegmented FeCo/Cu nanowires: electrosynthesis, characterization, and magnetic control of biomolecule desorption *ACS Appl. Mater. Interfaces* **7** 7389–96
- [14] Gapin A I, Ye X-R, Chen L-I, Hong D and Sungho J 2007 Patterned media based on soft/hard composite nanowire array of Ni/CoPt *IEEE Trans. Magn.* **43** 2151–3
- [15] Tanaka T, Matsuzaki J, Kurisu H and Yamamoto S 2008 Magnetization behavior of hard/soft-magnetic composite pillar *J. Magn. Mater.* **320** 3100–3
- [16] Allende S, Vargas N M, Altbir D, Vega V, Görlitz D and Nielsch K 2012 Magnetization reversal in multisegmented nanowires: parallel and serial reversal modes *Appl. Phys. Lett.* **101** 122412
- [17] Cisternas E and Vogel E E 2015 Improving information storage by means of segmented magnetic nanowires *J. Magn. Mater.* **388** 35–9
- [18] Evans P R, Yi G and Schwarzacher W 2000 Current perpendicular to plane giant magnetoresistance of multilayered nanowires electrodeposited in anodic aluminum oxide membranes *Appl. Phys. Lett.* **76** 481–3
- [19] Miltat J E and Donahue M J 2007 *Numerical Micromagnetics: Finite Difference Methods. Handbook of Magnetism and Advanced Magnetic Materials* (New York: Wiley)
- [20] Vazquez M and Vivas L G 2011 Magnetization reversal in Co-base nanowire arrays *Phys. Status Solidi b* **248** 2368–81
- [21] Aharoni A 1996 *Introduction to the Theory of Ferromagnetism* (Oxford: Oxford University Press)
- [22] Brown W F 1963 Thermal fluctuations of a single-domain particle *Phys. Rev.* **130** 1677–86
- [23] Aharoni A 1997 Angular dependence of nucleation by curling in a prolate spheroid *J. Appl. Phys.* **82** 1281–7
- [24] Frei E H, Shtrikman S and Treves D 1957 Critical size and nucleation field of ideal ferromagnetic particles *Phys. Rev.* **106** 446–55
- [25] Kronmüller H and Fähnle M 2003 *Micromagnetism and the Microstructure of Ferromagnetic Solids* (Cambridge: Cambridge University Press)
- [26] Lavin J, Denardin J C, Escrig J, Altbir D, Cortés A and Gómez H 2009 Angular dependence of magnetic properties in Ni nanowire arrays *J. Appl. Phys.* **106** 103903
- [27] Landeros P, Allende S, Escrig J, Salcedo E, Altbira D and Vogel E E 2007 Reversal modes in magnetic nanotubes *Appl. Phys. Lett.* **90** 102501
- [28] Escrig J, Bachmann J, Jing J, Daub M, Altbir D and Nielsch K 2008 Crossover between two different magnetization reversal modes in arrays of iron oxide nanotubes *Phys. Rev. B* **77** 214421
- [29] Hertel R and Kirschner J 2004 Magnetization reversal dynamics in nickel nanowires *Physica B* **343** 206–10
- [30] Forster H, Schrefl T, Scholz W, Suess D, Tsiantos V and Fidler J 2002 Micromagnetic simulation of domain wall motion in magnetic nano-wires *J. Magn. Mater.* **249** 181–6
- [31] De La Torre J, Piroux L, Olais J M and Encinas A 2010 Double ferromagnetic resonance and configuration-dependent dipolar coupling in unsaturated arrays of bistable magnetic nanowires *Phys. Rev. B* **81** 144411
- [32] Kou X, Fan X, Dumas R K, Lu Q, Zhang Y, Zhu H, Zhang X, Liu K and Xiao J Q 2011 Memory effect in magnetic nanowire arrays *Adv. Mater.* **23** 1393–7
- [33] Nielsch K, Choi J, Schwirn K, Wehrspohn R B and Gösele U 2002 Self-ordering regimes of porous alumina: the 10 porosity rule *Nano Lett.* **2** 677–80
- [34] Clime L, Ciureanu P and Yelon A 2006 Magnetostatic interactions in dense nanowire arrays *J. Magn. Mater.* **297** 60–70
- [35] Clime L, Zhao S Y, Chen P, Normandin F, Roberge H and Veres T 2007 The interaction field in arrays of ferromagnetic barcode nanowires *Nanotechnology* **18** 435709
- [36] Hertel R 2001 Micromagnetic simulations of magnetostatically coupled Nickel nanowires *J. Appl. Phys.* **90** 5752–8
- [37] Zighem F, Mauer T, Ott F and Chaboussant G 2011 Dipolar interactions in arrays of ferromagnetic nanowires: a micromagnetic study *J. Appl. Phys.* **109** 013910
- [38] Navau C, Chen D-X, Sanchez A and Del-Valle N 2011 Demagnetizing effects in granular hard magnetic bodies *J. Appl. Phys.* **109** 093901
- [39] Ivanov Y P, Vázquez M and Chubykalo-Fesenko O 2013 Magnetic reversal modes in cylindrical nanowires *J. Phys. D: Appl. Phys.* **46** 485001
- [40] Agramunt-Puig S, Del-Valle N, Navau C and Sanchez A 2014 Controlling vortex chirality and polarity by geometry in magnetic nanodots *Appl. Phys. Lett.* **104** 012407
- [41] Stoner E C and Wohlfarth E P 1948 A mechanism of magnetic hysteresis in heterogeneous alloys *Phil. Trans. R. Soc. London A* **240** 599–642
- [42] Ravea W, Ramstöckb K and Hubert A 1998 Corners and nucleation in micromagnetics *J. Magn. Mater.* **183** 329–33
- [43] Aharoni A 2001 Micromagnetics: past, present and future *Physica B* **306** 1–9
- [44] Guslienko K Y 1999 Magnetostatic interdot coupling in two-dimensional magnetic dot arrays *Appl. Phys. Lett.* **75** 394–6